ENGENHARIA E CIÊNCIAS TÉRMICAS
9th BRAZILIAN CONGRESS OF THERMAL ENGINEERING AND SCIENCES

Paper CIT02-0221

FINITE ELEMENT SUPG PARAMETERS COMPUTED FROM LOCAL MATRICES FOR COMPRESSIBLE FLOWS

Lucia Catabriga
Department of Computer Science (DI)
Federal University of Espírito Santo (UFES)
Av. Fernando Ferrari, s/n, Goiabeiras, 29060-900, Vitória, ES, Brazil
luciac@inf.ufes.br

Alvaro L. G. A. Coutinho
Department of Civil Engineering - COPPE
Federal University of Rio de Janeiro (UFRJ)
Caixa Postal 68506, 21945 970, Rio de Janeiro, RJ, Brazil
alvaro@nacad.ufrj.br

Tayfun E. Tezduyar
Mechanical Engineering, Rice University – MS 321
6100 Main Street, Houston, Texas 77005, USA
tezduyar@rice.edu

Abstract. *We present, for the SUPG formulation of inviscid compressible flows, stabilization parameters defined based on the element-level matrices. These definitions are expressed in terms of the ratios of the norms of the relevant matrices. They take into account the flow field, the local length scales, and the time step size. We compare the performance of these stabilization parameters, accompanied by a shock-capturing parameter introduced earlier, with the performance of a stabilization parameter introduced earlier, accompanied by the same shock-capturing parameter. We investigate the performance difference between updating the stabilization and shock-capturing parameters at the end of every time step and at the end of every nonlinear iteration within a time step. We also investigate the influence of activating an algorithmic option that was introduced earlier, which is based on freezing the shock-capturing parameter at its current value when a convergence stagnation is detected.*

Key Words: *Euler equations, compressible flow, finite elements, element-by-element data structures, stabilization parameter*

1. Introduction

Some of the most well-established and widely-used stabilized formulations in finite element flow computations are the streamline-upwind/Petrov-Galerkin (SUPG) formulation for incompressible flows (Hughes and Brooks, 1979), SUPG formulation for compressible flows (Tezduyar and Hughes, 1982; Tezduyar and Hughes, 1983), and pressure-stabilizing/Petrov-Galerkin (PSPG) formulation for incompressible flows (Tezduyar, 1991). The SUPG and PSPG formulations prevent numerical oscillations and other instabilities in solving problems with high Reynolds and/or Mach numbers and shocks and strong boundary layers, as well as when using equal-order interpolation functions for velocity and pressure and other unknowns. They act without introducing excessive numerical dissipation. Because its symptoms are not necessarily qualitative, excessive numerical dissipation is not always easy to detect. This concern makes it desirable to seek and employ stabilized formulations developed with objectives that include keeping numerical dissipation to a minimum. It was pointed out in Tezduyar et al., 1993 that these stabilized formulations also substantially improve the convergence rate in iterative solution of the large, matrix systems. Such matrix systems are solved at every Newton-Raphson step in iterative solution of the coupled nonlinear equation systems generated at every time level of a simulation.

The SUPG formulation for incompressible flows was first introduced in Hughes and Brooks, 1979. The SUPG formulation for compressible flows was first introduced, in the context of conservation variables, in a NASA Technical Report by Tezduyar and Hughes, 1982 and an AIAA paper by Tezduyar and Hughes, 1983. After that, several SUPG-like methods for compressible flows were developed. Taylor-Galerkin method (Donea, 1984), for example, is very similar, and under certain conditions is identical, to one of the SUPG methods introduced in Tezduyar and Hughes, 1982 and Tezduyar and Hughes, 1983. Another example of the subsequent SUPG-like methods for compressible flows in conservation variables is the streamline-diffusion method described

in Johnson et al., 1984. Later, following Tezduyar and Hughes, 1982 and Tezduyar and Hughes, 1983, the SUPG formulation for compressible flows was recast in entropy variables and supplemented with a shock-capturing term (Hughes et al., 1987). It was shown in ASME paper by Le Beau and Tezduyar, 1991 that, the SUPG formulation introduced in Tezduyar and Hughes, 1982 and Tezduyar and Hughes, 1983, when supplemented with a similar shock-capturing term, is very comparable in accuracy to the one that was recast in entropy variables. Later, 2D test computations for inviscid flows reported by Le Beau et al., 1993 showed that the SUPG formulation in conservation and entropy variables yielded indistinguishable results.

The PSPG formulation for the Navier-Stokes equations of incompressible flows, introduced in Tezduyar, 1991, assures numerical stability while allowing us to use equal-order interpolation functions for velocity and pressure. An earlier version of this stabilized formulation for Stokes flow was reported in Hughes et al., 1986. A recently introduced SUPG formulation for compressible flows in augmented conservation variables (Mittal and Tezduyar, 1998) leads to a proper incompressible flow formulation in the limit as the Mach number is taken to zero.

A stabilization parameter that is almost always known as "τ" is embedded in the SUPG and PSPG formulations. Careful selection of τ plays an important role in determining the accuracy of the formulation. This parameter involves a measure of the local length scale (also known as "element length") and other parameters such as the local Reynolds and Courant numbers. Various element lengths and τs were proposed starting with those in Hughes and Brooks, 1979 and Tezduyar and Hughes, 1982 and Tezduyar and Hughes, 1983 , followed by the one introduced in Tezduyar and Park, 1986, and those proposed in the subsequently reported SUPG and PSPG methods. In this paper, we will call the SUPG formulation introduced in NASA Technical Report Tezduyar and Hughes, 1982 and AIAA paper by Tezduyar and Hughes, 1983 for compressible flows "$(SUPG)_{82}$", and the set of τs introduced in conjunction with that formulation "τ_{82}". The stabilized formulation introduced in Tezduyar and Park, 1986 for advection-diffusion-reaction equations included a shock-capturing term and a τ definition that takes into account the interaction between that shock-capturing term and the SUPG term. That τ definition, for example, precludes "compounding" (i.e. augmentation of the SUPG effect by the shock-capturing effect when the advection and shock directions coincide). The τ used in Le Beau and Tezduyar, 1991 with $(SUPG)_{82}$ is a slightly modified version of τ_{82}. A shock-capturing parameter, which we will call in this paper "δ_{91}", was embedded in the shock-capturing term used in Le Beau and Tezduyar, 1991. Subsequent minor modifications of τ_{82} took into account the interaction between the shock-capturing and the $(SUPG)_{82}$ terms in a fashion similar to how it was done in Tezduyar and Park, 1986 for advection-diffusion-reaction equations. All these slightly modified versions of τ_{82} have always been used with the same δ_{91}, and we will categorize them in this paper all under the label "$\tau_{82\text{-MOD}}$".

Recently, new ways of computing the τs based on the element-level matrices and vectors were introduced in Tezduyar and Osawa, 2000 in the context of the advection-diffusion equation and the Navier-Stokes equations of incompressible flows. These new definitions are expressed in terms of the ratios of the norms of the relevant matrices or vectors. They automatically take into account the local length scales, advection field and the element-level Reynolds number. Based on these definitions, a τ can be calculated for each element, or even for each element node or degree of freedom or element equation. It was also shown in Tezduyar and Osawa, 2000 that these τs, when calculated for each element, yield values quite comparable to those calculated based on the definition introduced in Tezduyar and Park, 1986. In conjunction with these stabilization parameters, in Tezduyar, 2001, a Discontinuity-Capturing Directional Dissipation stabilization was introduced as a potential alternative or complement to the LSIC (least-squares on incompressibility constraint) stabilization. A second element length scale based on the solution gradient was also introduced in Tezduyar, 2001. This new element length scale would be used together with the element length scales already defined (directly or indirectly) in Tezduyar and Osawa, 2000. New stabilization parameters for the diffusive limit were introduced in Tezduyar, 2002. These new parameters are closely related to the second element length scale that was introduced in Tezduyar, 2001. That second element length scale can be recognized in Tezduyar, 2002 as a diffusion length scale.

It was pointed out in Tezduyar and Osawa, 2000 and Tezduyar, 2001 that the τs to be used in advancing the solution from time level n to $n+1$ (including the τ embedded in the LSIC stabilization term, which resembles a discontinuity-capturing term) should be evaluated at time level n (i.e. based on the flow field already computed for time level n), so that we are spared from another level of nonlinearity.

In this paper, we apply the τ definitions based on the element-level matrices to the $(SUPG)_{82}$ formulation introduced in Tezduyar and Hughes, 1982 and Tezduyar and Hughes, 1983 for inviscid compressible flows, supplemented with the shock-capturing term (with δ_{91}) introduced in Le Beau and Tezduyar, 1991. Our studies here include performance comparisons between these τs (with δ_{91}) and a $\tau_{82\text{-MOD}}$ (with δ_{91}) and comparisons between evaluating these τs and δ_{91} at time level n and at (every nonlinear iteration of) time level $n+1$. We also here test the influence of activating the convergence-detection δ_{91}-freezing option introduced in Catabriga and Coutinho, 2002. With that option, when a convergence stagnation is detected, δ_{91} is frozen at its current value.

2. Euler Equations

The system of conservation laws governing inviscid, compressible fluid flow are the Euler equations. These equations, restricted to two spatial dimensions, may be written in terms of conservation variables $\mathbf{U} = (\rho, \rho u, \rho v, \rho e)$, as

$$\mathbf{U}_{,t} + \mathbf{F}_{x,x} + \mathbf{F}_{y,y} = \mathbf{0} \quad \text{on} \quad \Omega \times [0,T] \tag{1}$$

where $\mathbf{F}_x$ and $\mathbf{F}_y$ are the Euler fluxes given elsewhere Hirsh, 1992, Ω is a domain in $\mathbb{R}^2$ and T is a positive real number. We denote the spatial and temporal coordinates respectively by $\mathbf{x} = (x,y) \in \overline{\Omega}$ and $t \in [0,T]$, where the superimposed bar indicates set closure, and Γ is the boundary of domain Ω. Here ρ is the fluid density; $\mathbf{u} = (u_x, u_y)^T$ is the velocity vector; e is the total energy per unit mass. We add to equation (1) the ideal gas assumption, relating pressure with the total energy per unit mass and kinetic energy. Alternatively, equation (1) may be written as,

$$\mathbf{U}_{,t} + \mathbf{A}_x \mathbf{U}_{,x} + \mathbf{A}_y \mathbf{U}_{,y} = \mathbf{0} \quad \text{on} \quad \Omega \times [0,T] \tag{2}$$

where $\mathbf{A}_i = \frac{\partial \mathbf{F}_i}{\partial \mathbf{U}}$. Associated to equation (2) we have proper boundary and initial conditions.

3. Stabilized formulation and stabilization parameters

Considering a standard discretization of Ω into finite elements, the $(SUPG)_{82}$ formulation for the Euler equations in conservation variables introduced by Tezduyar and Hughes, 1982 and Tezduyar and Hughes, 1983 is written as,

$$\begin{aligned} \int_\Omega \mathbf{W}^h . \left(\frac{\partial \mathbf{U}^h}{\partial t} + \mathbf{A}_i^h \frac{\partial \mathbf{U}^h}{\partial x_i} \right) d\Omega \quad + \\ \sum_{e=1}^{n_{el}} \int_{\Omega^e} \boldsymbol{\tau} \mathbf{A}_k^h \left(\frac{\partial \mathbf{W}^h}{\partial x_k} \right) . \left[\frac{\partial \mathbf{U}^h}{\partial t} + \mathbf{A}_i^h \frac{\partial \mathbf{U}^h}{\partial x_i} \right] d\Omega \quad + \\ \sum_{e=1}^{n_{el}} \int_{\Omega^e} \delta_{91} \frac{\partial \mathbf{W}^h}{\partial x_i} . \frac{\partial \mathbf{U}^h}{\partial x_i} d\Omega \quad = \quad 0 \end{aligned} \tag{3}$$

where $\mathbf{W}^h$ and $\mathbf{U}^h$, respectively the discrete weighting and test functions, are defined on standard finite element spaces. In (3) the first integral corresponds to the Galerkin formulation, the first series of element-level integrals are the SUPG stabilization terms, and the second series of element-level integrals are the shock-capturing terms added to the variational formulation to prevent spurious oscillations around shocks. The shock-capturing parameter, δ_{91}, is evaluated here using the approach proposed by Le Beau and Tezduyar, 1991,

$$\delta_{91} = \left[\frac{\| \mathbf{A}_x^h \frac{\partial \mathbf{U}^h}{\partial x} + \mathbf{A}_y^h \frac{\partial \mathbf{U}^h}{\partial y} \|^2_{\tilde{\mathbf{A}}_0^{-1}}}{\| \frac{\partial \xi}{\partial x} \frac{\partial \mathbf{U}^h}{\partial x} + \frac{\partial \xi}{\partial y} \frac{\partial \mathbf{U}^h}{\partial y} \|^2_{\tilde{\mathbf{A}}_0^{-1}} + \| \frac{\partial \eta}{\partial x} \frac{\partial \mathbf{U}^h}{\partial x} + \frac{\partial \eta}{\partial y} \frac{\partial \mathbf{U}^h}{\partial y} \|^2_{\tilde{\mathbf{A}}_0^{-1}}} \right]^{\frac{1}{2}} \tag{4}$$

We define the following element-level matrices:

$$\mathbf{m} : \int_{\Omega^e} \mathbf{W}^h \frac{\partial \mathbf{U}^h}{\partial t} d\Omega \tag{5}$$

$$\tilde{\mathbf{c}} : \int_{\Omega^e} \left(\mathbf{A}_x^h \frac{\partial \mathbf{W}^h}{\partial x} . \frac{\partial \mathbf{U}^h}{\partial t} + \mathbf{A}_y^h \frac{\partial \mathbf{W}^h}{\partial y} . \frac{\partial \mathbf{U}^h}{\partial t} \right) d\Omega \tag{6}$$

$$\mathbf{c} : \int_{\Omega^e} \left(\mathbf{W}^h . \mathbf{A}_x^h \frac{\partial \mathbf{U}^h}{\partial x} + \mathbf{W}^h . \mathbf{A}_y^h \frac{\partial \mathbf{U}^h}{\partial y} \right) d\Omega \tag{7}$$

$$\tilde{\mathbf{k}} : \int_{\Omega^e} \left(\mathbf{A}_x^h \frac{\partial \mathbf{W}^h}{\partial x} . \mathbf{A}_x^h \frac{\partial \mathbf{U}^h}{\partial x} + \mathbf{A}_x^h \frac{\partial \mathbf{W}^h}{\partial x} . \mathbf{A}_y^h \frac{\partial \mathbf{U}^h}{\partial y} + \mathbf{A}_y^h \frac{\partial \mathbf{W}^h}{\partial y} . \mathbf{A}_x^h \frac{\partial \mathbf{U}^h}{\partial x} + \mathbf{A}_y^h \frac{\partial \mathbf{W}^h}{\partial y} . \mathbf{A}_y^h \frac{\partial \mathbf{U}^h}{\partial y} \right) d\Omega \tag{8}$$

Considering the standard finite element approximation we have:

$$\mathbf{U}^h = \mathbf{N}\mathbf{v} \tag{9}$$

$$\mathbf{W}^h = \mathbf{N}\mathbf{c} \tag{10}$$

$$\mathbf{U}_{,t}^h = \mathbf{N}\mathbf{a} \tag{11}$$

where $\mathbf{v}$ is the vector of nodal values of $\mathbf{U}$ (depending on time only), $\mathbf{c}$ is a vector of arbitrary constants, $\mathbf{a}$ is the time derivate of the $\mathbf{v}$ ($\mathbf{a} = \frac{d\mathbf{v}}{dt}$) and $\mathbf{N}$ is a matrix containing the space dependent shape functions. Restricting ourselves to linear triangles, the element shape functions may be represented in matrix form as,

$$\mathbf{N}^e = \left[\begin{array}{ccc} N_1\mathbf{I} & N_2\mathbf{I} & N_3\mathbf{I} \end{array} \right] \tag{12}$$

where N_1, N_2 e N_3 are the element shape functions and $\mathbf{I}$ is the identity matrix of order 4. The shape functions for linear triangles in natural coordinates are:

$$N_1 = \xi \quad N_2 = \eta \quad N_3 = 1 - \xi - \eta \tag{13}$$

It is useful to define the discrete local (element) gradient operator as,

$$\mathbf{B} = \left[\begin{array}{c} \mathbf{B}_x \\ \mathbf{B}_y \end{array} \right] = \left[\begin{array}{c} \frac{\partial \mathbf{N}}{\partial x} \\ \frac{\partial \mathbf{N}}{\partial y} \end{array} \right] \tag{14}$$

Then, we may write $\mathbf{B}_x$ and $\mathbf{B}_y$ for the linear triangle as,

$$\mathbf{B}_x = \frac{1}{2A^e} \left[\begin{array}{ccc} y_{23}\mathbf{I} & y_{31}\mathbf{I} & y_{12}\mathbf{I} \end{array} \right] \tag{15}$$

$$\mathbf{B}_y = \frac{1}{2A^e} \left[\begin{array}{ccc} x_{32}\mathbf{I} & x_{13}\mathbf{I} & x_{21}\mathbf{I} \end{array} \right] \tag{16}$$

where A^e is the area of the element, $x_{ij} = x_i - x_j$, and $y_{ij} = y_i - y_j$ for $i, j = 1, 2, 3$. Substituting the above relations into the weak formulation and proceeding in the standard manner we may arrive to the element matrices:

$$\mathbf{m} = \int_{\Omega e} \mathbf{N}^T \mathbf{N} d\Omega^e \tag{17}$$

$$\mathbf{m} = \frac{A^e}{12} \left[\begin{array}{ccc} 2\mathbf{I} & \mathbf{I} & \mathbf{I} \\ \mathbf{I} & 2\mathbf{I} & \mathbf{I} \\ \mathbf{I} & \mathbf{I} & 2\mathbf{I} \end{array} \right] \tag{18}$$

$$\tilde{\mathbf{c}} = \int_{\Omega e} (\mathbf{B}_x^T \mathbf{A}_x^h \mathbf{N} + \mathbf{B}_y^T \mathbf{A}_y^h \mathbf{N}) d\Omega^e \tag{19}$$

$$\tilde{\mathbf{c}} = \frac{1}{6} \begin{bmatrix} \mathbf{m}^1 & \mathbf{m}^1 & \mathbf{m}^1 \\ \mathbf{m}^2 & \mathbf{m}^2 & \mathbf{m}^2 \\ \mathbf{m}^3 & \mathbf{m}^3 & \mathbf{m}^3 \end{bmatrix} \tag{20}$$

where $\mathbf{m}^1$, $\mathbf{m}^2$ and $\mathbf{m}^3$ are given by,

$$\begin{aligned} \mathbf{m}^1 &= y_{23}\mathbf{A}_x + x_{32}\mathbf{A}_y \\ \mathbf{m}^2 &= y_{31}\mathbf{A}_x + x_{13}\mathbf{A}_y \\ \mathbf{m}^3 &= y_{12}\mathbf{A}_x + x_{21}\mathbf{A}_y \end{aligned} \tag{21}$$

$$\mathbf{c} = \int_{\Omega e} (\mathbf{N}^T \mathbf{A}_x \mathbf{B}_x + \mathbf{N}^T \mathbf{A}_y \mathbf{B}_y) d\Omega^e \tag{22}$$

$$\mathbf{c} = \frac{1}{6} \begin{bmatrix} \mathbf{c}^1 & \mathbf{c}^2 & \mathbf{c}^3 \\ \mathbf{c}^1 & \mathbf{c}^2 & \mathbf{c}^3 \\ \mathbf{c}^1 & \mathbf{c}^2 & \mathbf{c}^3 \end{bmatrix} \tag{23}$$

and the submatrices $\mathbf{c}^1$, $\mathbf{c}^2$ and $\mathbf{c}^3$ are,

$$\begin{aligned}\mathbf{c}^1 &= y_{23}\mathbf{A}_x + x_{32}\mathbf{A}_y \\ \mathbf{c}^2 &= y_{31}\mathbf{A}_x + x_{13}\mathbf{A}_y \\ \mathbf{c}^3 &= y_{12}\mathbf{A}_x + x_{21}\mathbf{A}_y\end{aligned} \tag{24}$$

$$\tilde{\mathbf{k}} = \int_{\Omega^e} \mathbf{B}^T \begin{bmatrix} \mathbf{A}_x\mathbf{A}_x & \mathbf{A}_x\mathbf{A}_y \\ \mathbf{A}_y\mathbf{A}_x & \mathbf{A}_y\mathbf{A}_y \end{bmatrix} \mathbf{B} d\Omega^e \tag{25}$$

$$\tilde{\mathbf{k}} = \frac{1}{4A^e} \begin{bmatrix} \mathbf{B}_{11} & \mathbf{B}_{12} & \mathbf{B}_{13} \\ \mathbf{B}_{21} & \mathbf{B}_{22} & \mathbf{B}_{23} \\ \mathbf{B}_{31} & \mathbf{B}_{32} & \mathbf{B}_{33} \end{bmatrix} \tag{26}$$

The submatrices in Eq.(26) are:

$$\mathbf{B}_{12} = y_{23}(y_{31}\mathbf{A}_{xx} + x_{13}\mathbf{A}_{xy}) + x_{32}(y_{31}\mathbf{A}_{yx} + x_{13}\mathbf{A}_{yy}) \tag{27}$$
$$\mathbf{B}_{13} = y_{23}(y_{12}\mathbf{A}_{xx} + x_{21}\mathbf{A}_{xy}) + x_{32}(y_{12}\mathbf{A}_{yx} + x_{21}\mathbf{A}_{yy}) \tag{28}$$
$$\mathbf{B}_{21} = y_{31}(y_{23}\mathbf{A}_{xx} + x_{32}\mathbf{A}_{xy}) + x_{13}(y_{23}\mathbf{A}_{yx} + x_{32}\mathbf{A}_{yy}) \tag{29}$$
$$\mathbf{B}_{23} = y_{31}(y_{12}\mathbf{A}_{xx} + x_{21}\mathbf{A}_{xy}) + x_{13}(y_{12}\mathbf{A}_{yx} + x_{21}\mathbf{A}_{yy}) \tag{30}$$
$$\mathbf{B}_{31} = y_{12}(y_{23}\mathbf{A}_{xx} + x_{32}\mathbf{A}_{xy}) + x_{21}(y_{23}\mathbf{A}_{yx} + x_{32}\mathbf{A}_{yy}) \tag{31}$$
$$\mathbf{B}_{32} = y_{12}(y_{31}\mathbf{A}_{xx} + x_{13}\mathbf{A}_{xy}) + x_{21}(y_{31}\mathbf{A}_{yx} + x_{13}\mathbf{A}_{yy}) \tag{32}$$
$$\mathbf{B}_{11} = -(\mathbf{B}_{12} + \mathbf{B}_{13}) \tag{33}$$
$$\mathbf{B}_{22} = -(\mathbf{B}_{21} + \mathbf{B}_{23}) \tag{34}$$
$$\mathbf{B}_{33} = -(\mathbf{B}_{31} + \mathbf{B}_{32}) \tag{35}$$

where $\mathbf{A}_{ij} = \mathbf{A}_i\mathbf{A}_j$ for $i, j = x, y$. We define the SUPG parameters from the element matrices as given in Tezduyar and Osawa, 2000,

$$\tau_{S1} = \frac{\|\mathbf{c}\|}{\|\tilde{\mathbf{k}}\|} \tag{36}$$
$$\tau_{S2} = \frac{\|\mathbf{c}\|}{\|\tilde{\mathbf{c}}\|} \tag{37}$$
$$\tag{38}$$

where $\|.\| = max_{1\le i\le n_{ee}}\{|a_{i1}|+|a_{i2}|+\ldots+|a_{i,n_{ex}}|\}$, n_{ee} is the number of element equations, that is, the number of element nodes times the number of degrees of freedom per node. We define the resulting SUPG parameter, as given in Tezduyar and Osawa, 2000,

$$\tau_{SUPG} = \left(\frac{1}{\tau_{S1}^r} + \frac{1}{\tau_{S2}^r}\right)^{-1/r} \tag{39}$$

where r is an integer parameter.

4. Numerical Results

4.1. Oblique Shock

The first problem consists of a two-dimensional steady problem of a inviscid, Mach 2, uniform flow, over a wedge at an angle of $-10°$ with respect to a horizontal wall, resulting in the occurrence of an oblique shock with an angle of 29.3° emanating from the leading edge of the wedge, as shown in Figure 1.

The computational domain is the square $0 \le x \le 1$ and $0 \le y \le 1$. Prescribing the following flow data at the inflow, i.e., on the left and top sides of the shock, results in the exact solution with the flow data past the

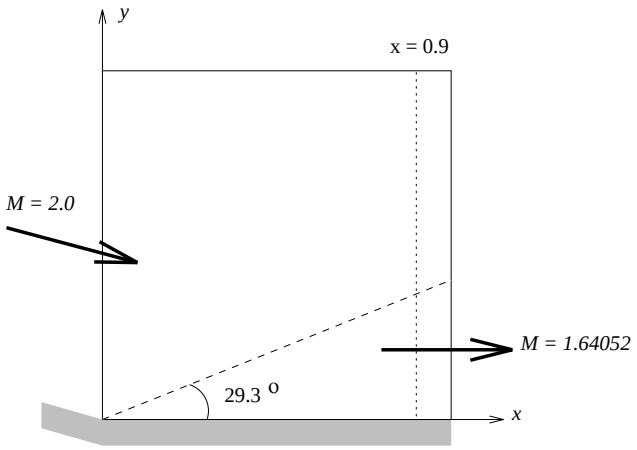

Figure 1: Oblique shock - problem description.

shock:

$$\text{Inflow} \begin{cases} M &= 2.0 \\ \rho &= 1.0 \\ u_1 &= cos10^0 \\ u_2 &= -sin10^0 \\ p &= 0.17857 \end{cases} \qquad \text{Outflow} \begin{cases} M &= 1.64052 \\ \rho &= 1.45843 \\ u_1 &= 0.88731 \\ u_2 &= 0.0 \\ p &= 0.30475 \end{cases} \tag{40}$$

where M is the Mach number, ρ is the flow density, u_1 and u_2 are the horizontal and vertical velocities respectively, and p is the pressure.

Four Dirichlet boundary conditions are imposed on the left and top boundaries; the slip condition $u_2 = 0$ is set at the bottom boundary; and no boundary conditions are imposed on the outflow (right) boundary. A 20×20 mesh with 800 linear triangles and 441 nodes is employed. Tolerance of preconditioned GMRES algorithm is set to 0.1, the dimension of the Krylov subspace to 5 and the number of multicorrections fixed to 3. All the solutions are initialized with free-stream values.

Figure 2(a) shows density along line $x = 0.9$, computed by a $\tau_{82\text{-MOD}}$ parameter and the new τ parameter with $r = 1, 2, 3$ and 5. Here we update τ and δ_{91} at every nonlinear iteration of a time level (i.e. iteration update). All solutions are very similar, therefore from now on we are going to use $r = 2$. Figure 2(b) shows the evolution of density residual for 300 steps.

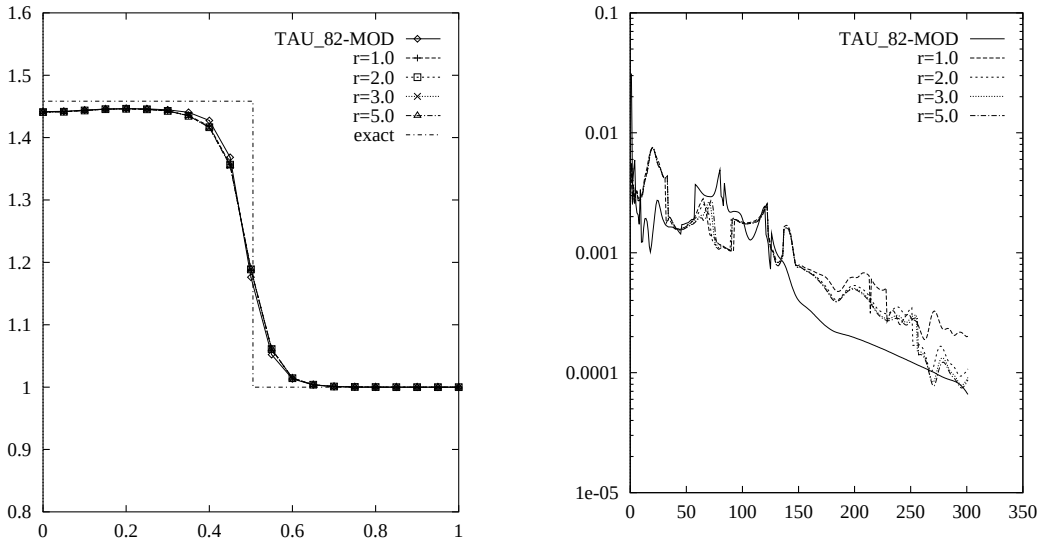

(a) Density profile at $x = 0.9$.

(b) Evolution of density residual.

Figure 2: Oblique shock - investigation about r parameter.

We also tested what happens if we update τ and δ_{91} only at every time step at the beginning of a time step

(i.e. time-step update). Figure 3(a) shows the density along line $x = 0.9$ with iteration update and time-step update. Both solutions are virtually identical. Figure 3(b) shows the evolution of the density residual for 300 steps. The evolution of density residual for time-step update is faster than iteration update.

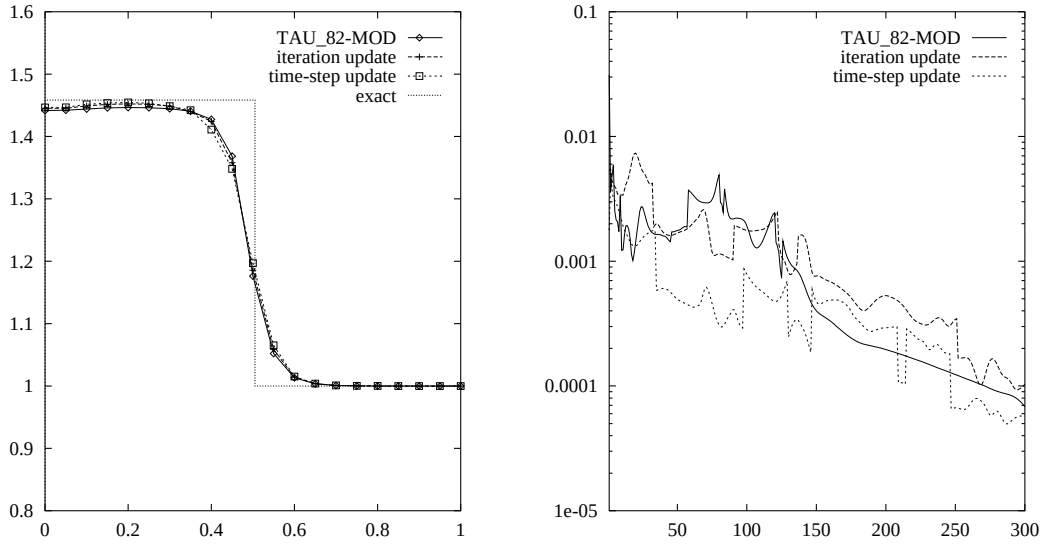

(a) Density profile at $x = 0.9$. (b) Evolution of density residual.

Figure 3: Oblique shock - investigation about updating.

Figures 4(a) and 4(b) show the action of Catabriga and Coutinho, 2002 procedure to detect convergence stagnation and afterwards freezing the contribution of the shock-capturing parameter, with the two updating strategies for τ and δ_{91}. The density profiles computed with the convergence stagnation procedure switched on are very similar to the previous cases as well as the evolution of density residual. However, when we update τ only at every time step we observe that a few more GMRES iterations are needed compared to when we update τ every nonlinear iteration. The exact number of iterations for both cases are respectively 4,879 and 4,798 and these figures are better than the number of GMRES iterations obtained by the standard procedure to compute τ and δ_{91}, that is, 5,226 GMRES iterations.

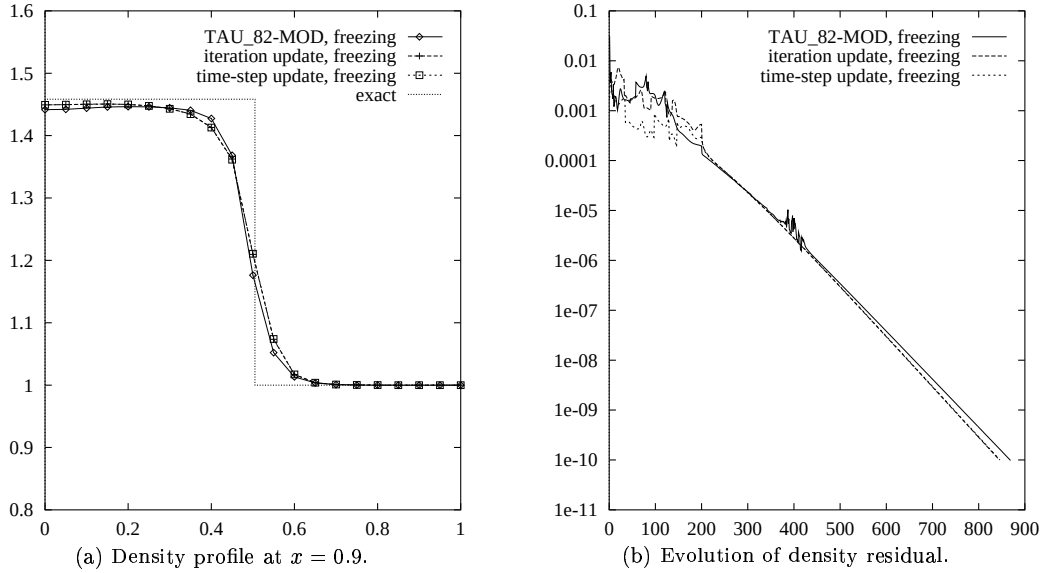

(a) Density profile at $x = 0.9$. (b) Evolution of density residual.

Figure 4: Oblique shock - freezing shock capturing.

4.2. Reflected Shock

This two-dimensional steady problem consists of three regions (R1, R2 and R3) separated by an oblique shock and its reflection from a wall, as shown in Figure 5. Prescribing the following Mach 2.9 flow data at the

inflow, i.e., the first region on the left (R1), and requiring that the incident shock to be at an angle of 29°, leads to the exact solution (R2 and R3):

$$\text{R1}\begin{cases} M &= 2.9 \\ \rho &= 1.0 \\ u_1 &= 2.9 \\ u_2 &= 0.0 \\ p &= 0.714286 \end{cases} \quad \text{R2}\begin{cases} M &= 2.3781 \\ \rho &= 1.7 \\ u_1 &= 2.61934 \\ u_2 &= -0.50632 \\ p &= 1.52819 \end{cases} \quad \text{R3}\begin{cases} M &= 1.94235 \\ \rho &= 2.68728 \\ u_1 &= 2.40140 \\ u_2 &= 0.0 \\ p &= 2.93407 \end{cases} \tag{41}$$

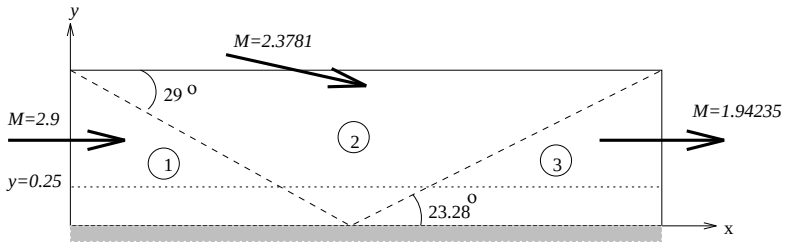

Figure 5: Reflected shock - problem description.

We prescribe density, velocities and pressure on the left and top boundaries; the slip condition is imposed on the wall (bottom boundary); and no boundary conditions are set on the outflow (right) boundary. We consider a structured mesh with 60×20 cells, where each cell was divided into two triangles (1281 nodes and 2400 elements) and an unstructured mesh with 1,837 nodes and 3,429 elements covering the domain $0 \leq x \leq 4.1$ and $0 \leq y \leq 1$. The tolerance of the preconditioned GMRES algorithm is 0.1, the dimension of the Krylov subspace is 5, the number of multi-corrections is 3, and all the solutions are initialized with free-stream values.

Figure 6(a) shows the density along line $y = 0.25$ for the structured mesh, computed by a $\tau_{82\text{-MOD}}$ parameter and the new τ parameter with $r = 2$, for iteration update and time-step update cases. As in the previous problem, both solutions are very similar. Figure 6(b) shows the evolution of density residual for 300 steps. We observe that the density residual computed updating τ and δ_{91} with time-step update is smaller than the one computed by the other alternative strategies.

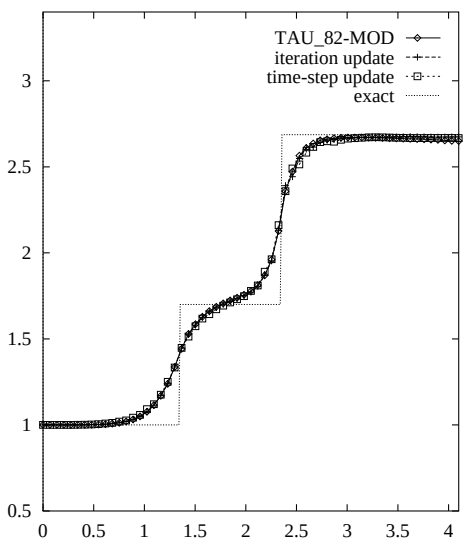

(a) Density profile at $y = 0.25$.

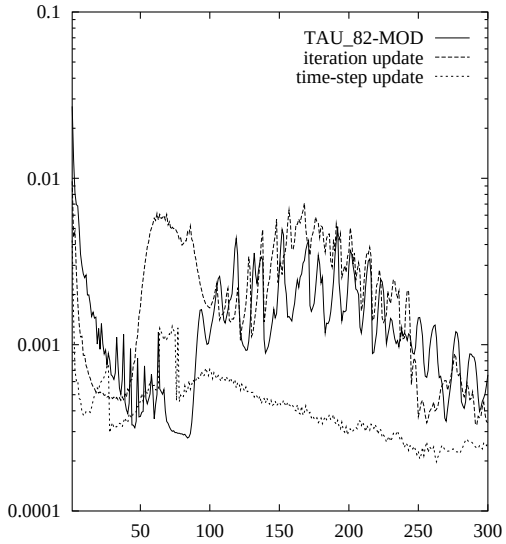

(b) Evolution of density residual.

Figure 6: Reflected shock - structured mesh - investigation about updating.

Figures 7(a) and 7(b) show the action of the convergence stagnation detection procedure, with the two updating strategies for τ and δ_{91}. The density profiles computed with the convergence stagnation procedure switched on are very similar to the previous cases. However, here $\tau_{82\text{-MOD}}$ lead to a better evolution of the density residual, needing 3,226 GMRES iterations. For the cases when we update τ with time-step update we observe 3,627 GMRES iterations and for the case when we update τ with iteration update we needed 3,787 GMRES iterations.

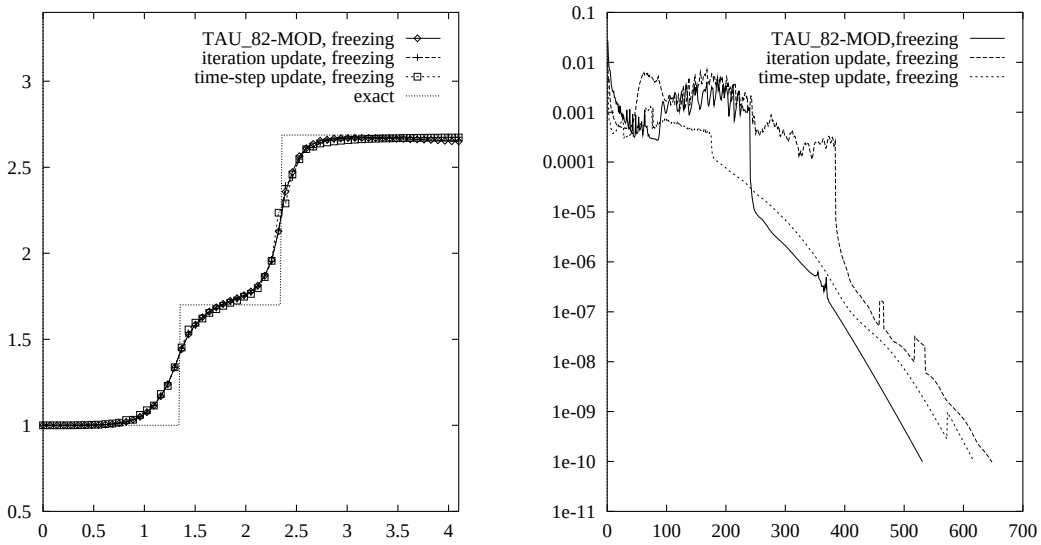

(a) Density profile at $y = 0.25$.

(b) Evolution of density residual.

Figure 7: Reflected shock - structured mesh - freezing shock capturing.

Figure 8 shows the density contours for the unstructured mesh, computed by using the same τs and updating strategies of the previous case. Again, all solutions are very similar. Figure 9 shows the evolution of density residual for 300 steps for iterations update and time-step update. We observe that the density residual diminishes significantly faster for the case where τ and δ_{91} are updated only at every time-step.

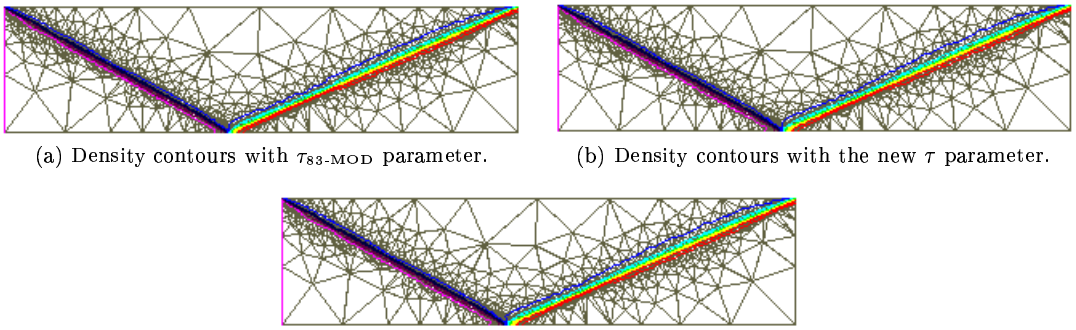

(a) Density contours with $\tau_{83\text{-MOD}}$ parameter.

(b) Density contours with the new τ parameter.

(c) Density contours with the new τ parameter and without updating.

Figure 8: Reflected shock - density contours in the unstructured mesh.

The action of the convergence stagnation detection procedure can be observed in Figures 10 and 11. We see that the steady-state density distributions are in good agreement. Again in this problem the solution obtained with the $\tau_{82\text{-MOD}}$ reaches steady-state faster, as shown in Figure 11. Note that the $\tau_{82\text{-MOD}}$ solution reaches steady-stated in 836 steps, needing 9,573 GMRES iterations, while for the case where parameters are update with iteration update and time-step update we need respectively 9,980 and 9,485 GMRES iterations.

5. Concluding remarks

We highlighted, for the SUPG formulation of inviscid compressible flows, stabilization parameters defined based the element element-level matrices. These definitions are expressed in terms of the ratios of the norms of the relevant matrices, and take automatically into account the flow field, the local length scales, and the time step size. By inspecting the solution quality and convergence history, we compared the performance of these stabilization parameters, accompanied by a shock-capturing parameter introduced earlier, with the performance of a stabilization parameter introduced earlier, accompanied by the same shock-capturing parameter. Also by inspecting the solution quality and convergence history, we investigated the performance difference between updating the stabilization and shock-capturing parameters at the end of every time step and at the end of every nonlinear iteration within a time step. We observed that the solution qualities were quite comparable. Updating the new stabilization parameters at the end of every time step gives better convergence than updating them at

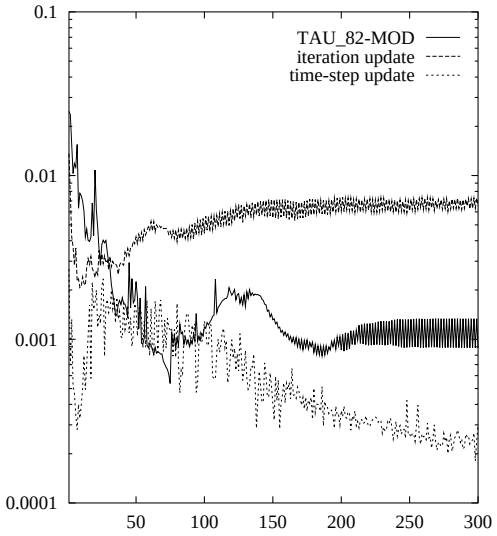

Figure 9: Reflected shock - evolution of density residual in the unstructured mesh - investigation about updating.

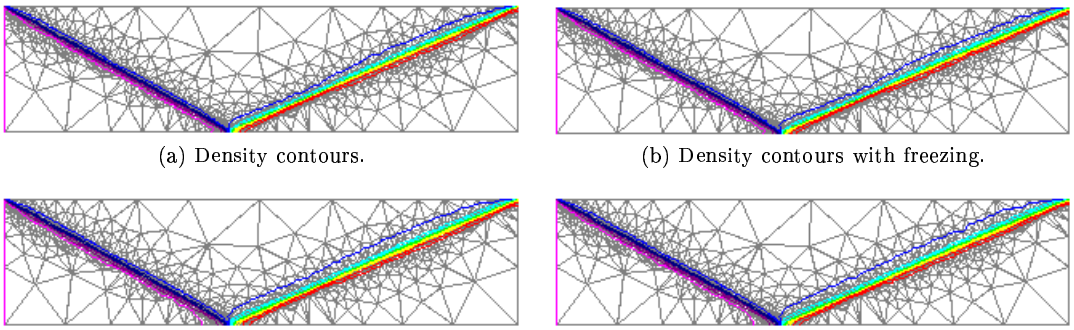

(a) Density contours.

(b) Density contours with freezing.

(c) Density contours without updating.

(d) Density contours without updating and with freezing.

Figure 10: Reflected shock - density contours in the unstructured mesh - freezing shock-capturing.

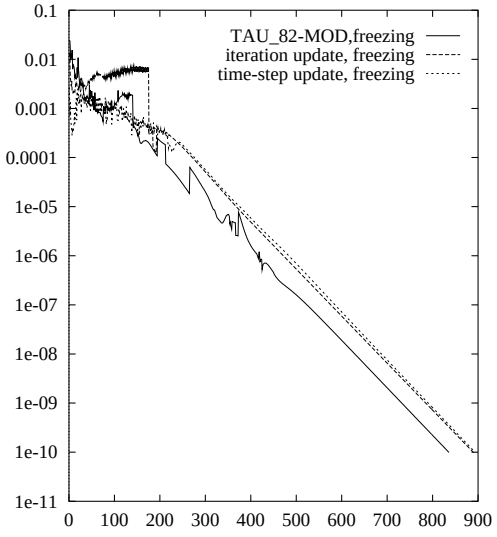

Figure 11: Reflected shock - evolution of density residual in the unstructured mesh - freezing shock capturing.

the end of every nonlinear iteration. We also investigated the influence of activating an algorithmic option that was introduced earlier, which is based on freezing the shock-capturing parameter at its current value when a convergence stagnation is detected. From the convergence histories in that investigation, we observe that this freezing option benefits both the older and newer definitions of the stabilization parameters, with a slightly more benefit for the older definition.

6. Acknowledgments

This work is partly supported by grant CNPq/PROTEM-CC 68.0066/01-2 and CNPq/MCT 522692/95-8. The third author was supported by the US Army Natick Soldier Center and NASA.

7. References

Catabriga, L. and Coutinho, A., 2002, Improving convergence to steady-state of implicit SUPG solution of Euler equations, "Communications in Numerical Methods in Engineering", Vol. 18, pp. 345–353.

Donea, J., 1984, A Taylor-Galerkin method for convective transport problems, "International Journal for Numerical Methods in Engineering", Vol. 20, pp. 101–120.

Hirsh, C., 1992, "Numerical Computation of Internal and External Flows - Computational Methods for Inviscid and Viscous Flows, Vol. 2", John Wiley and Sons Ltd, Chichester.

Hughes, T. and Brooks, A., 1979, A multi-dimensional upwind scheme with no crosswind diffusion, Hughes, T., editor, "Finite Element Methods for Convection Dominated Flows", Vol. 34, pp. 19–35, New York. ASME.

Hughes, T., Franca, L., and Balestra, M., 1986, A new finite element formulation for computational fluid dynamics: V. Circumventing the Babuška–Brezzi condition: A stable Petrov–Galerkin formulation of the Stokes problem accommodating equal-order interpolations, "Computer Methods in Applied Mechanics and Engineering", Vol. 59, pp. 85–99.

Hughes, T., Franca, L., and Mallet, M., 1987, A new finite element formulation for computational fluid dynamics: VI. Convergence analysis of the generalized SUPG formulation for linear time-dependent multi-dimensional advective-diffusive systems, "Computer Methods in Applied Mechanics and Engineering", Vol. 63, pp. 97–112.

Johnson, C., Navert, U., and Pitkaranta, J., 1984, Finite element methods for linear hyperbolic problems, "Computer Methods in Applied Mechanics and Engineering", Vol. 45, pp. 285–312.

Le Beau, G., Ray, S., Aliabadi, S., and Tezduyar, T., 1993, SUPG finite element computation of compressible flows with the entropy and conservation variables formulations, "Computer Methods in Applied Mechanics and Engineering", Vol. 104, pp. 397–422.

Le Beau, G. J. and Tezduyar, T. E., 1991, Finite element computation of compressible flows with the SUPG formulation, Dhaubhadel, M., Engelman, M., and Reddy, J., editors, "Advances in Finite Element Analysis in Fluid Dynamics", Vol. 123, pp. 21–27, New York. ASME.

Mittal, S. and Tezduyar, T., 1998, A unified finite element formulation for compressible and incompressible flows using augumented conservation variables, "Computer Methods in Applied Mechanics and Engineering", Vol. 161, pp. 229–243.

Tezduyar, T., 1991, Stabilized finite element formulations for incompressible flow computations, "Advances in Applied Mechanics", Vol. 28, pp. 1–44.

Tezduyar, T., 2001, Adaptive determination of the finite element stabilization parameters, "European Congress on Computational Methods in Applied Sciences and Engineering-ECCOMAS Computational Fluid Dynamics Conference CD-ROM", pp. 1–13, Swansea, Wales, UK.

Tezduyar, T., 2002, Stabilized finite element formulations and interface-tracking and interface-capturing techniques for incompressible flows, "to appear in *Proceedings of the Workshop on Numerical Simulations of Incompressible Flows*", Half Moon Bay, California.

Tezduyar, T., Aliabadi, S., Behr, M., Johnson, A., and Mittal, S., 1993, Parallel finite-element computation of 3D flows, "IEEE Computer", Vol. 26, pp. 27–36.

Tezduyar, T. and Hughes, T., 1982, Development of Time-accurate Finite Element Techniques for First-order Hyperbloic Systems with Particular Emphasis on the Compressible Euler Equations, NASA Technical Report NASA-CR-204772, NASA.

Tezduyar, T. and Hughes, T., 1983, Finite element formulations for convection dominated flows with particular emphasis on the compressible Euler equations, "21st Aerospace Sciences Meeting", Vol. 83-0125, Reno, Nevada. AIAA.

Tezduyar, T. and Osawa, Y., 2000, Finite element stabilization parameters computed from element matrices and vectors, "Computer Methods in Applied Mechanics and Engineering", Vol. 190, pp. 411–430.

Tezduyar, T. and Park, Y., 1986, Discontinuity capturing finite element formulations for nonlinear convection-diffusion-reaction problems, "Computer Methods in Applied Mechanics and Engineering", Vol. 59, pp. 307–325.